Applied Clay Science 176 (2019) 21–28

Contents lists available at ScienceDirect

Applied Clay Science

journal homepage: www.elsevier.com/locate/clay

Research paper

A novel method for surface wettability modification of talc through thermal treatment

Hao Yi[a,b], Yunliang Zhao[a,b,*], Yiping Liu[b], Wei Wang[b], Shaoxian Song[a,b,*], Cheng Liu[b], Hongqiang Li[c], Weiquan Zhan[b], Xin Liu[d]

[a] Hubei Key Laboratory of Mineral Resources Processing and Environment, Wuhan University of Technology, 122 Luoshi Road, Wuhan, Hubei 430070, China
[b] School of Resources and Environmental Engineering, Wuhan University of Technology, 122 Luoshi Road, Wuhan, Hubei 430070, China
[c] School of Xingfa Mining Engineering, Wuhan Institute of Technology, Wuhan, Hubei 430205, China
[d] Qingdao Top Biotechnology Co. LTD, 72 Liaoyang East Road, Qingdao, Shandong 266101, China

ARTICLE INFO

Keywords:
Surface wettability
Modification
Siloxane
Amorphous silica
Thermal treatment
Talc

ABSTRACT

Silica tetrahedron (also called siloxane) is an important structure of clay minerals, the percentage of which influences the hydrophobicity, polarity and other surface properties on clay mineral surfaces. In this study, a novel method for surface wettability modification of talc through thermal treatment has been put forward. In this method, the symmetrical siloxane structures on talc basal surfaces were broken by transforming the non-polar siloxane structure into a polar structure during the thermal treatment process, thus to decrease the hydrophobic components on talc surfaces, and therefore achieve the goal of surface wettability modification. This study was performed through the measurements of thermosgravimetric analysis and differential scanning calorimetry (TG-DSC), contact angle and wetting heat measurements, fourier transform infrared spectroscopy (FTIR), and ^{29}Si-nuclear magnetic resonance spectroscopy (^{29}Si NMR) as well as molecular dynamic simulations (MDs). The results indicate that the thermal treatment at 960 °C for only a very short time could greatly decrease the contact angle of water on talc surfaces. The mechanism could be attributed to that the thermal treatment leads to the disorder of some of the Si—O bond length and O-Si-O bond angle in talc silica tetrahedron structure, which finally results in the disorder of the symmetrical siloxane structure and the formation of the amorphous silica phase. And the decrease of hydrophobic siloxane structures on talc surface gives rise to the relatively strong hydrophilicity on talc surfaces. This current method improves the wettability of talc without any addition of modifiers, which would be helpful of many applications of clay minerals, such as clay-polymer composites, filler materials, clay mineral dispersion in aqueous suspensions or mineral processing, etc.

1. Introduction

Talc, as a typical clay mineral, has numberous applications due to its specific properties such as thermal stability, hydrophobicity, organophilicity and adsorption properties (Claverie et al., 2018). Traditionally, talc has been extensively applied as fillers in industrial process such as papermaking, ceramics, wall materials, plastics, rubber, paints and cosmetics (Andrić et al., 2014; Fonseca et al., 2015). Recently, clay minerals have shown enormous potentials in preparing nanocomposite materials and functions materials with excellent properties, such as flame retardant materials (Bonati et al., 2013; Pack et al., 2010), electrode materials (Adpakpang et al., 2016), environment fucntion materials (Kang et al., 2018; Li and Peng, 2018a, 2018b) and drug delivery materials (Zhang et al., 2016, 2017). Despite that talc was found to be hydrophilic and showed increased affinity to water molecules when degassed at 100–400 °C, it was still hydrophobic in its natural state (Michot et al., 1994). Besides, some studies have found that talc was hydrophilic at low relative humidity while it showed hydrophobicity when at saturation (Rotenberg et al., 2011). In this work, talc was considered as macroscopically hydrophobic due to the natural floatability and very poor dispersion (Liu et al., 2019b). Talc particles with strong hydrophobicity are difficult to disperse in aqueous solutions, which are detrimental to the application of talc (Yi et al., 2018b). For example, in papermaking industry, the chemically inert talc leads to a poor fiber-to-filler bonding, which results in a poor properties of paper (Polowczyk and Kozlecki, 2017; Samyn, 2013). In

* Corresponding authors at: Hubei Key Laboratory of Mineral Resources Processing and Environment, Wuhan University of Technology, 122 Luoshi Road, Wuhan, Hubei 430070, China.
E-mail addresses: zyl286@whut.edu.cn (Y. Zhao), ssx851215@whut.edu.cn (S. Song).

https://doi.org/10.1016/j.clay.2019.04.023
Received 14 September 2018; Received in revised form 11 April 2019; Accepted 20 April 2019
Available online 28 April 2019
0169-1317/

the field of ceramics, the non-uniform mixtures of clay and others constituents have adverse impact on the mechanical properties of ceramics (Okada et al., 2009; Ptáček et al., 2014). In mineral processing, similar wettability of clays and other minerals results in a poor flotation separation performance (Liu et al., 2019a, 2019c). As for composite materials, the compatibility between clay minerals and other components also affects the specific functional performances of composite mateials (Li et al., 2018; Peng et al., 2016; Wang et al., 2018a).

Therefore, it is necessary to modify the surface wettability of talc particles in order to improve their compatibility, especially at this current time that clay minerals are playing more and more significant role in materials area such as composites and two-dimension nano materials (Barcelos et al., 2018; Wang et al., 2018b; Yi et al., 2019). Thus surface wettability modification for clay minerals are desperately needed and then these specific structural minerals can be better taken advantege in materials. And some strategies have been introduced to modify surface wettability, commonly used wettability modification method is achieved by addition of modifiers such as surfactants and polymers (Kaggwa et al., 2006; Krysztafkiewicz and Domka, 1997; K. Liu et al., 2016a,b). In these existing surface modification technologies, the contacts between the talc particles and modifiers are bad. Colloidal clay minerals usually aggregate into large flocs (Chen et al., 2017), thus many clay particles inside the flocs have no chance to contact with the modifiers when being in modified stage, resulting in a part of clay particles not being modified. In consequence, talc particles are generally not modified uniformly, which severely restricted the application of clay minerals.

Considering that modification of wetting properties of clay minerals is required in many applications, an attempt has been tried to introduce a newly surface modification method thus to overcome non-uniformity problem in existing modification process. It is well-known that the 1:1 layered clay minerals consist of the repetition of one tetrahedral and one octahedral sheet, while one octahedral sheet is sandwiched between two tetrahedral sheets in the 2:1 layered clay minerals (Brigatti et al., 2006; Underwood et al., 2016). What is particularly attractive in clay mineral structure is the highly symmetrical and non-polar silica tetrahedron structure (also called siloxane) (Xian et al., 2017). Studies have showed that the neutral siloxane surfaces composed of silica tetrahedron, such as talc (001) surfaces and pyrophyllite (001) surfaces, are the most nonreactive surface in all the surfaces of clay mineral (Nalaskowski et al., 2007; Schoonheydt and Johnston, 2006; Wallqvist et al., 2006). The apical oxygen atoms in the silica tetrahedron structure are very weak electron donors, which has been turned out to interact with water molecules very weakly (Schoonheydt and Johnston, 2006). The basal surface wettability of kaolin, including the siloxane surface and the hydroxyl surface, have been investigated through molecular simulations, and the siloxane surface showed a microscopic contact angle of about 105° while the water droplets are fully wetting the octahedral hydroxyl surface (Šolc et al., 2011). Besides, the strong adsorption of hydrophobic aromatic hydrocarbons from water demonstrated the hydrophobicity nature of siloxane surface in smectites (Jaynes and Boyd, 1991). Hence, the siloxane structure was proved to be inactive, nonpolar and hydrophobic practically and theoretically. The edge surface of talc is of hydrophilicity due to the broken bonds, while the basal surface (001) is of strong hydrophobicity due to exposure of siloxane plane (Yehia and Al-Wakeel, 2000). Thus it is the hydrophobic siloxane structure, exposed on both basal surfaces of talc, that determined the hydrophobic nature of talc particles due to the very little percentage of edge surfaces. The wettability of layered talc particles is dominant by the basal surface consist of siloxane structure, which provides the theoretically possibility to modify the surface wettability by breaking the symmetrical siloxane structure.

As mentioned above, talc contains the relatively ideal dimensions of siloxane sheet in the (001) plane, which leads to the strong hydrophbocity of talc surface. Therefore, breaking the symmetrical siloxane structure on talc basal surface may be an excellent way to change polarity of talc surface thus to modify the surface wettability. According to some previous studies, some phase changes of talc may occurr to the crystal talc structure under high temperature. *Richar Ward* has investigated the kinetics of the dehydroxylation of talc by means of isothermal weight-change determinations (Richard Ward, 1975). Besides, the dehydroxylation and structure changes in heated talc has been studied by NMR spectroscopy (MacKenzie and Meinhold, 1994) and infrared spectroscopy (Zhang et al., 2006). A literature review has aslo been presented concerning the application of thermoanalytical methods for the examination of thermal decomposition of talc (Wesolowski, 1984). Also, controlled transtormation rate thermal analysis (CRTA) has been used to study the thermal decomposition of a talc sample and found two main decomposition steps at 500–650 °C and 650–1000 °C (Belgacem et al., 2008). Some fundamental insights into the effect of thermal behaviors on talc and kinetic analysis of the decomposition of talc under high temperature has been studied, which showed that the talc was decomposed with the formation of enstatite and amorphous silica (Liu et al., 2014). Therefore, previous studies have found that the decompostion of talc were accomponied with the transformation of siloxane into amorphous silica. Thus thermal treatment may lead to the structure changes on the siloxane structure and therefore can be used as an surface wettablity modification method. Based on this hypothesis, an attempt was made to destroy the symmetric siloxane structure through thermal treatment method and to modify the surface wettability of talc. For instance, by destroying a part of the siloxane structure in silica tetrahedron plane through previous reported thermal treatment, the surface wettability, surface energy, surface reactivity and so on can be altered due to the transformation of hydrophobic siloxane into hydrophilic amorphous silica.

Despite that some existing literatures have presented the effect of thermal treatment on the phase changes of talc powder, the improved effect of thermal treatment on the surface wettablity of talc have not been tested yet. Therefore, the wettability behaviors of talc powder before and after thermal treatment have been studied. In addition, a surface wettability modification method has been put forward based on the thermal treatment methods. Compare to previous modification method, this thermal treatment modification method, without adding any additional modifiers, is an easy and fast way to uniformly modify the surface wettability of talc particles. Hence, the main goals of this work are to investigate the wettability of talc before and after thermal treatment and then introduce a new method to modify surafce wettability through thermal treatment, and to reveal its mechanisms thus to provide a comprehensive understanding of the surface modification process.

2. Experiments

2.1. Raw materials and characterizations

Raw talc powders were obtained from Aladdin Industrial Corporation, phase composition of this material was determined by a D8 Advance X-ray diffractometer (XRD) (Bruker, Germany) with Cu-Kα radiation. And the surface morphology as well as the size of talc particles was observed by using a S4800 scanning electron microscope (SEM) (Hitachi, Japan).

2.2. Characterizations for thermal treatment

In the thermal treatment process, a certain amount of talc particles was put in ceramic crucible firstly, then this crucible was placed into a muffle furnace with the model of Vulcan 3–550 (Addlestone, Surrey, UK). The temperature inside the muffle furnace was heated up to 960 °C from room temperature in air, and the heating rate is 10 °C·min^{-1}. All the talc sample were thermal treated at 960 °C for a certain time ranged from 0 to 12.5 min. Subsequently, these calcined talc products were cooled in air, these resulted products were used to measure the contact

angle thus to investigate the surface wettability of talc sample before and after thermal treatment.

In order to investigate the thermal decomposition property of talc, thermogravimetry (TG) and differential scanning calorimetry (DSC) measurements were carried out in air, with the heating rate of 10 °C·min^{-1}, by using sta409pc equipment (Netzsch, Germany). Middle infrared transmission spectra in the range of 400 to 4000 cm^{-1} was determined by using a Thermo Scientific Nicolet 6700 FTIR spectrometer (Thermo Nicolet, USA) to study the structure changes of talc before and after heated. ^{29}Si nuclear magnetic resonance spectra (^{29}Si NMR) were obtained by using a NMR spectroscopy (Bruker AVANCE III, American) at 79.49 MHZ to investigate the siloxane structure alteration before and after calcined. A KBr-pressed technique was used to prepare talc sample for FTIR measurements, and the talc powder were directly used to measure XRD, SEM, TG-DSC and ^{29}Si NMR without further operation.

2.3. Characterizations for surface wettability modifications

The contact angles of the calcined talc products were determined by using a K100 surface tension meter (Kruss, Germany) at room temperature, according to the Wilhelmy plate method, thus to characterize the surface wettability of talc powder before and after calcination. In contact angle measurement, 0.5 g talc powder were pressed to a plate under 25 MPa by using a YLJ-15 T … t press machine (KJ GROUP, China). The temperature and relative humidity for contact angle measurements were 20 °C and 70% RH, respectively. In addition, the dispersion test has also been carried out to observe the dispersion properties of talc particles before and after thermal treatment. In this test, talc powders before and after thermal treatment were put in aqueous solution, and images of the dispersion behaviors of talc in aqueous solutions has been captured to study the surface wettability differences between the raw and calcined talc. Furthermore, the wetting heat of talc and calcined talc in water has also been measured to verify the modification of surface wettability. The heat of wetting is measured with SETARAM C80 Micro Calorimeter, talc and calcined talc without further operation were placed in sample cell and then being isothermal scanned by the micro calorimeter. All the water used in this work were ultra-pure water with electrical resistivity of 18.2 MΩ·cm, which were distilled and deionized by Millipore Super Q system (Millipore, America).

2.4. Molecular dynamic simulations

In this work, molecular simulation has also been performed to investigate the variation of the microstructure of talc (Ulian and Valdrè, 2015). The Forcite module in Materials studio package was applied to study the structure changes of talc at high temperature. First, the talc model was built according to previous study (Du and Miller, 2007; Larentzos et al., 2007), after which it was optimized based on the CLAYFF force field (Cygan et al., 2004; Yi et al., 2018a). And then molecular dynamics (MD) were performed to simulate microstructure changes under the condition of high temperature. These MD simulations were run in NPT ensemble for 5 ns to fully equilibrate the talc system (Yi et al., 2016). The potential energy was evaluated with a 15 Å cutoff for the short-range van der Waals interaction, and the Ewald summation method was used to calculate the long-range Coulombic interactions. After MD simulations, bond length distribution and bond angle distribution were analyzed to characterize the variation of microstructure and surface properties.

3. Results and discussion

3.1. Surface wettability modification of talc through thermal treatment

Generally, in clay mineral structure, it contains adsorbed water molecules (H_2O) and structural water molecules (-OH). When under thermal treatment, water molecules are being removed in different stages because of different bonding energy between water molecules and clay minerals. As shown in Fig. 1, the TG-DSC curves of the talc sample indicated that the weight loss of talc took place in three stages. In the first stage (①), a small weight loss and a endothermic DSC peak were observed due to the removal of the physically adsorbed water. This adsorption water only accounts for about 1% of the total talc mass. The next stage occurred when heated to 600–700 °C (②), the constitution water (OH groups) were partly driven off in this stage accompanied by a small endothermic effect. During the third stage (③), it displays an enormous loss of mass and a great endothermic effect, which corresponds to the liberation of the remaining structure water between 900 and 1100 °C. The loss of mass occupies approximately 4% in this stage. From the TG-DSC curve, the main reaction is the dehydration in the heating process, and these decomposition results are in accord with previous study (MacKenzie and Meinhold, 1994; Pérez-Maqueda et al., 2008). The first stage was the only removal of physical adsorbed water molecules, and the mainly dehydration of structure water process is being observed in the third dehydration stage when heated to 900–1050 °C. The removal of structural components may lead to the breakage of structural symmetry of talc, thus the thermal treatment temperature at 960 °C, around the endothermic peak in the third dehydration process, were chosen to treat with talc particles for surface modification.

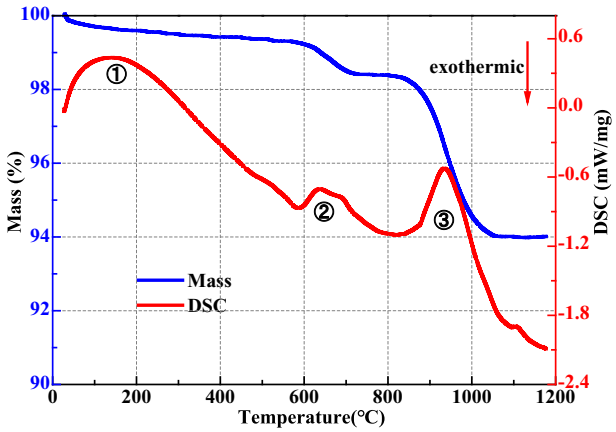

Fig. 1. TG-DSC curves of the talc sample.

In order to study the surface wettability changes before and after thermal treatment, the contact angle of talc treated by calcination for various time has been determined. Fig. 2 shows the contact angles of talc products being thermal treated with different times. The contact angle of the raw talc is 68.87°, which is consistent with many previous studies (Mierczynska-Vasilev and Beattie, 2013; Wallqvist et al., 2006). When calcined for 12.5 min, the contact angle of talc decrease to 55.34° from 68.87°. In conclusion, with talc being heated at 960 °C, the contact angle decreases with increasing calcination time. During thermal treatment, the hydrophilic groups such as hydroxyl are being removed little by little, but the surfaces becomes more hydrophilic gradually. It is interesting that the calcined talc becomes more hydrophilic while the hydrophilic hydroxyl groups are removed. Therefore, one possibility was inferred as the decrease of hydrophobic components such as siloxane structures. Meanwhile, since siloxane content mainly determines the surface wettability of talc, the decrease of contact angle values stands for the decrease of the amount of siloxane on talc surface qualitatively.

It is to be noted that the measured contact angle of talc strongly depends on the compactness, slab surface morphology and the porosity. In this work, we have applied a very high pressure (25 MPa) to try to produce a very compact talc slab with very smooth surface, and the

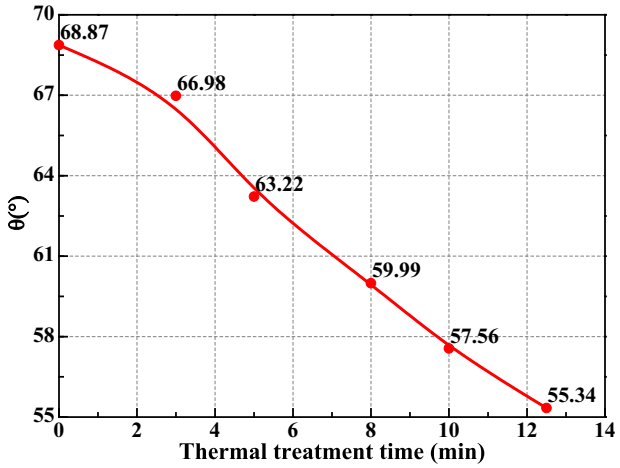

Fig. 2. Contact angle of talc products as a function of thermal treatment time.

measured contact angle of talc in this work (68.87°) is in agreement with many previous literatures. Besides, all the talc slabs are compressed under the same conditions, so that all the talc slabs are believed to be in similar compactness, roughness and porosity. As a result, the tendency that contact angle of talc decreases with increasing calcination time is believed to be convincing. Besides, the measured value does not represent the contact angle of a cleaved basal surface of talc because our talc are powder samples. And the measurement of contact angle of powder sample is usually Wilhelmy plate method, which may provide the average surface wettability of the whole powder. It is hard to determine the contact angle of a certain cleaved basal surface of a powder sample. The measured average surface wettability can also demonstrate the surface wettability changes before and after thermal treatment.

The wetting process often involves liquid spreading on solid surface and energy change, thus wetting phenomena and thermal effect are comprehensive representations of solid surface wettability (Liu et al., 2016). A higher wetting heat value indicates a stronger interaction between wetting agent and solid surfaces (Zhang and Wang, 2014). Except contact angle, heat of wetting ΔH has also been used to provide a characterization of surface wettability. As shown in Fig. 3, a great difference is found in the wetting heat between raw talc and calcined talc. The wetting heat value of talc and heated talc are -0.416 mW/g and -0.777 mW/g, respectively. The larger released heat in the wetting of calcined talc demonstrates the stronger interaction between treated talc and water. Thus, it is verified that calcined talc is easier to be wetted than raw talc. It is clear that the thermal treatment modified the surface wettability of talc due to the different wetting behaviors.

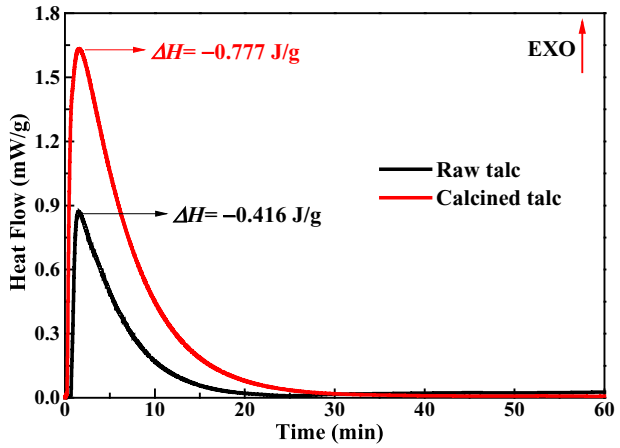

Fig. 3. Wetting heat of raw talc and calcined talc.

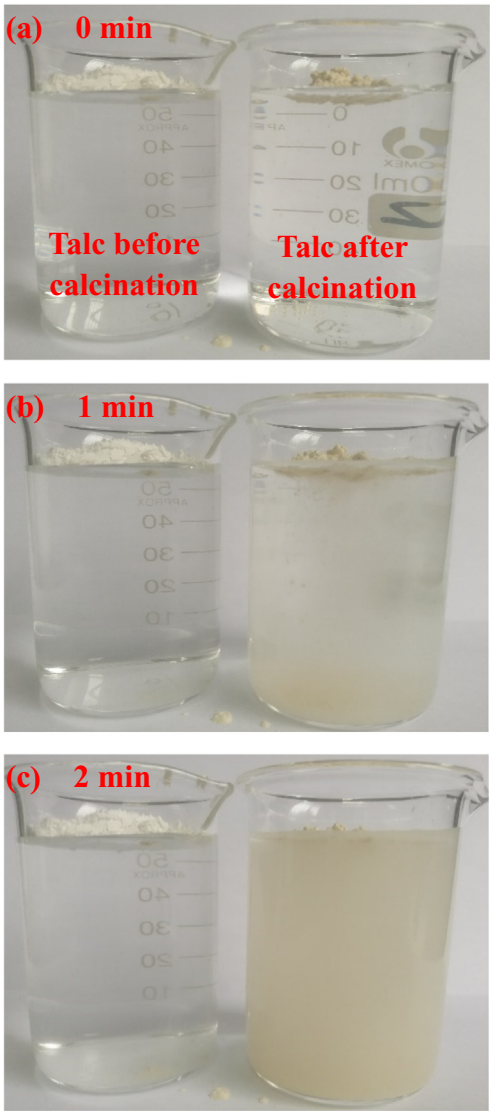

Fig. 4. Dispersion property of talc before (a) and after thermal treatment(b-c).

Therefore, this wetting heat measurements also turned out the successful surface wettability modification of talc particles after thermal treatment. The results of wetting heat measurement are in agreement with contact angle measurements, showing the same conclusion that the talc becomes less hydrophobic after calcination treatment.

For further verification of the surface modification results, dispersion property experiments have been carried out. The dispersion results of talc powder before and after thermal treatment in aqueous solution were shown in Fig. 4. For the raw talc powder, all the talc particles float on water due to the very strong hydrophobicity and the very small particle size. Even after a long time, the talc particles have not dispersed into the aqueous solutions. As for the talc powder after being thermal treated 10 min, the talc particles can directly disperse in water even without stirring. After sedimentation for 2 min, most of the talc particles dispersed into the aqueous solution spontaneously. It is obvious that talc particles became hydrophilic due to the easily dispersion property in aqueous solution after thermal treatment. The dispersion differences in this experiment provided another evidence for the enhancement of hydrophilicity of talc after thermal treatment. Combined with the contact angle results, it was demonstrated that surface wettability of talc can be modified through thermal treatment.

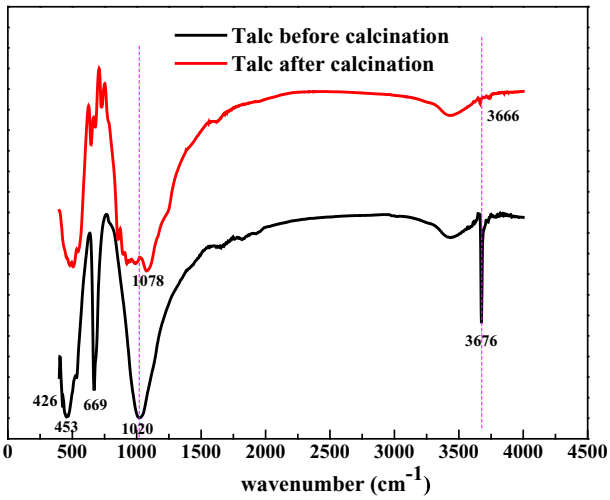

Fig. 5. FTIR spectra of talc sample before and after thermal treatment.

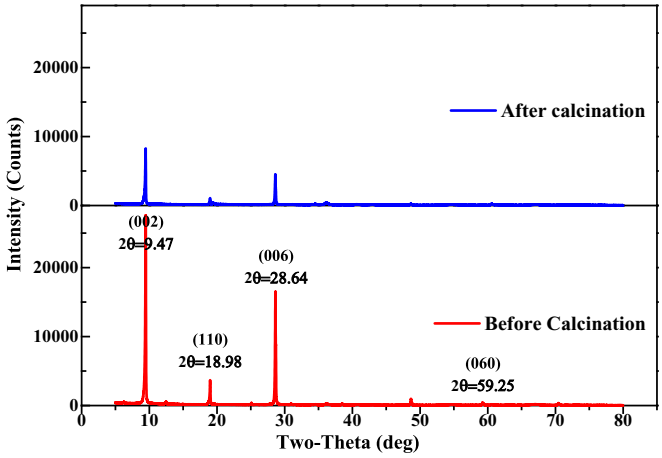

Fig. 6. XRD patterns of the talc sample before and after thermal treatment.

3.2. Characterizations of talc sample before and after thermal treatment

The FTIR spectra of talc sample revealed the variation of talc structure after calcined at 960 °C, shown in Fig. 5. According to previous study (Jamil and Palaniandy, 2011), the peak at 669 cm^{-1} was related to the stretching vibration of Mg—O, the peak at 426, 453, and 1020 cm^{-1} were originated from vibrations of Si—O bond in silica tetrahedron. Two obvious changes of FTIR spectra for talc were taken place after thermal treatment. First, the peak at 3676 cm^{-1} was on account of the stretching vibration of hydroxyl group, and it is obvious that dehydroxylation occurs in the heating process due to the disappearance of OH stretching vibration of talc after calcination. Then, the position shifted from 1020 cm^{-1} to 1078 cm^{-1} after calcination was attributed to the formation of amorphous silica from siloxane, which is consistent with previous study (Belgacem et al., 2008; Liu et al., 2014). Combined with the TG-DSC results, it could be concluded that the transformation of silica tetrahedron to amorphous silica took place gradually accompanied by dehydroxylation, which perfectly explained the decrease of contact angle of talc after thermal treatment. When calcined, the siloxane structure on talc basal surface (001) transformed into amorphous silica, the symmetrical siloxane structure was broken and the nonpolar talc surface became polar, resulting to the enhancement of the hydrophilicity. With the increasing of thermal treatment time, more and more siloxane transformed into amorphous silica, the significant reduction of hydrophobic content of siloxane on talc surfaces led to the decrease of contact angle gradually.

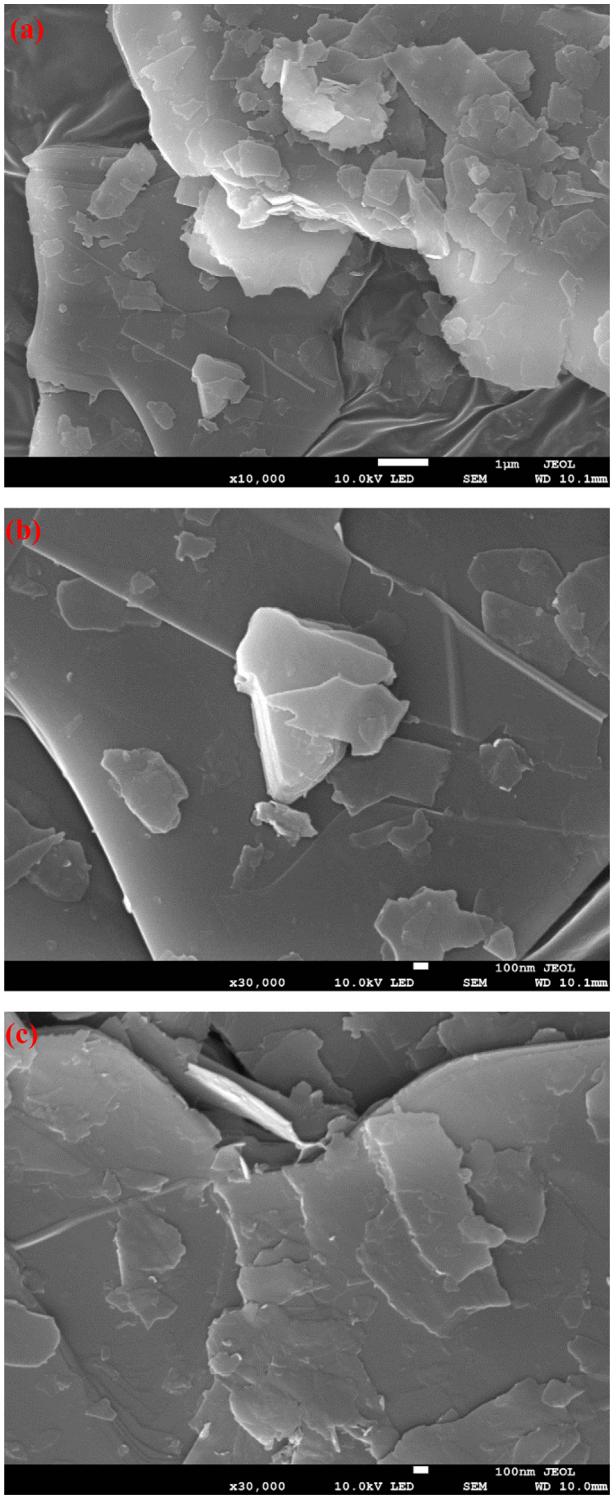

Fig. 7. SEM image of the talc sample before calcination (a-b) and after calcination (c).

Fig. 6 shows the XRD spectra of talc powder before and after thermal treatment. The diffraction peaks appear at 2θ = 9.47° (002), 18.98° (110), 28.64° (006) and 59.25° (060) well agree with the crystal structure of talc (Yang et al., 2006), indicating that the raw materials used in this work is talc. Besides, no impurities were observed, suggesting that the purity of raw talc powder is very high. The intensity and shape of the XRD reflections depend on the crystallinity, where more intense and narrower XRD reflections indicate a higher degree of

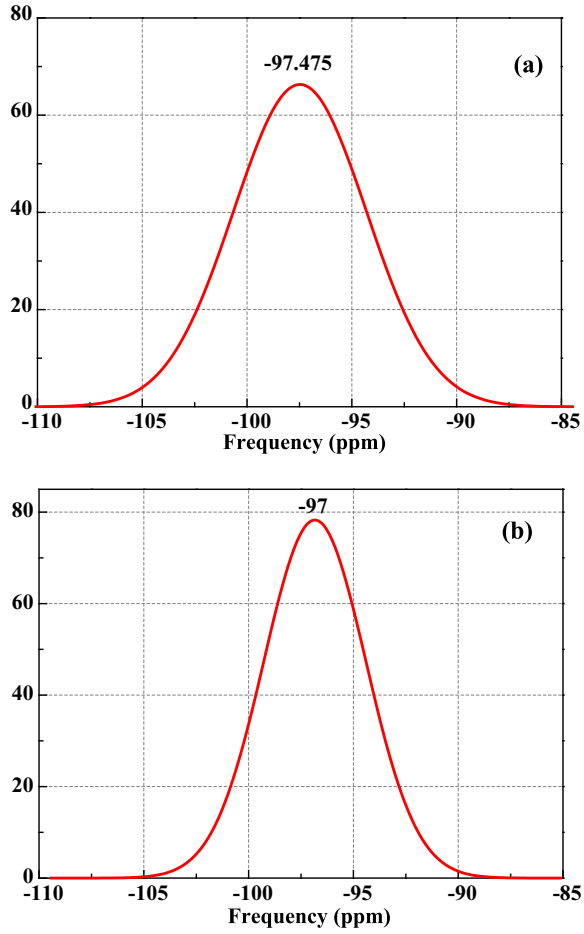

Fig. 8. ^{29}Si NMR spectra of talc before (a) and after thermal treatment (b).

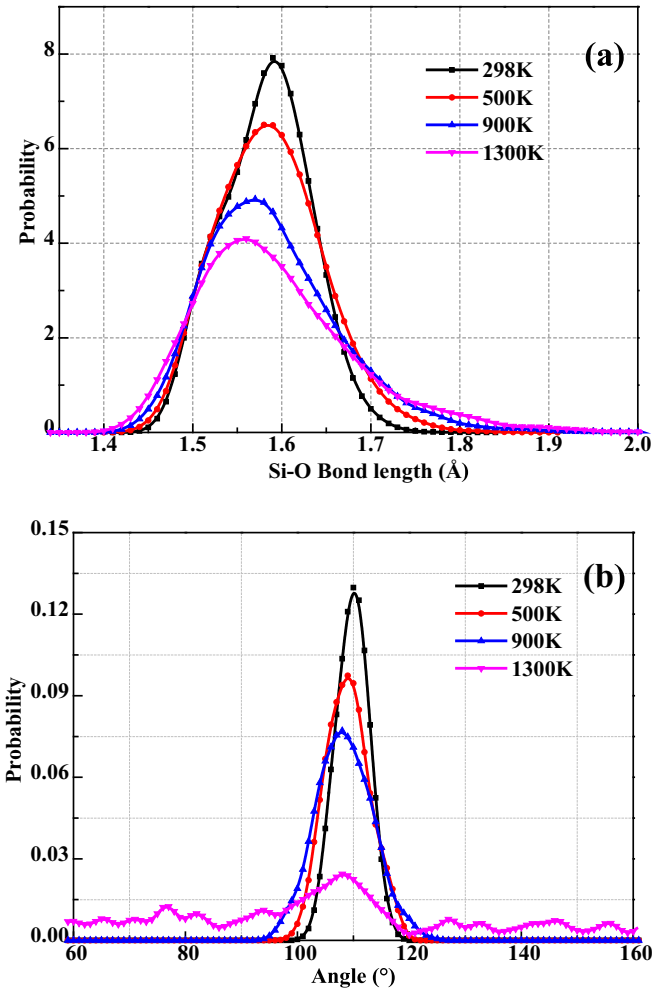

Fig. 9. Distribution of Si—O bond length (a) and O-Si-O angle (b) equilibrated at different temperature.

talc crystallinity. Compared with the XRD pattern of raw talc powder, the not very high intense XRD reflections of talc after thermal treatment indicates the increase of amorphous degree, which is in agreement with the results of FTIR.

The surface morphology and particle size of talc was observed through SEM image, as shown in Fig. 7. The size of talc is as large as several micrometers. Besides, the morphology of raw talc appears in shape of flake, indicating that the basal (001) surfaces accounts for the most of the outer surfaces of talc while the hydrophilic edge surfaces occupy only a very small proportion. Compared with the SEM image of talc before (Fig. 7b) and after thermal treatment (Fig. 7c), it is obvious that the surfaces of calcined talc are not smooth as that of raw talc. According to the FTIR results, it was found that the siloxane structure on talc surface transformed into amorphous silica. Combined with SEM images (Fig. 7b), the little rough surface of thermal treated talc may be caused by the formation of amorphous silica. Thus, this SEM image of thermal treated talc can also demonstrate the increase of amorphous degree.

The ^{29}Si NMR spectra of talc before and after calcination has also been determined to investigate structure variation of talc, the results of which are shown in Fig. 8. The spectrum of unheated talc, with a chemical shift of 97.475 ppm, is within the range of previously reported values (−97 to −98.1 ppm) (Borges et al., 2016; Lippmaa et al., 1980; MacKenzie and Meinhold, 1994). When heated to 960 °C, the spectrum of the calcined talc still has a peak at about −97.0 ppm (Fig. 7b), which still corresponds better to the talc structure. The negligible changes of the chemical shift in ^{29}Si NMR spectra provide evidence that the talc and calcined talc both are of Q3 phyllosilicate structure, indicating that the coordination number of Si still keep the same. Thus it turns out that, except for some siloxane sites being transformed into amorphous silica, no other structure changes have taken place in the heating process. These ^{29}Si NMR results are in accord with the SEM image of calcined talc, in which the shape of talc is still flake except the increase of roughness.

3.3. Molecular dynamic simulations

MDs were performed in order to verify the structure changes of talc structure at high temperature from a microscopic perspective. Fig. 9a and b display Si—O bond length distribution as well as O-Si-O bond angle distribution equilibrated at different temperature, respectively. It was found that, when at room temperature, the Si—O bond length distribution shows a peak at approximately 0.16 nm while the bond angle of Si-O-Si distribution displays a peak at nearly 110°. These results are in accordance with the bond length of Si—O and bond angle of O-Si-O in theory (Tesson et al., 2016). When at high temperature, the relatively sharp peak of Si—O bond length distribution (Fig. 9a) and O-Si-O bond angle distribution (Fig. 9b) becomes less sharp, indicating that the number of normal Si—O bond and O-Si-O bond angle in silica tetrahedron structures accord with experimental and theoretical results are decreasing. After thermal treatment, a small percentage of the Si—O bond length as well as Si-O-Si bond angle do not correspond to known crystalline siloxane structure in talc, demonstrating the destruction of some symmetrical siloxane structure in talc. This simulation results agree well with experimental studies and provide another proof for the

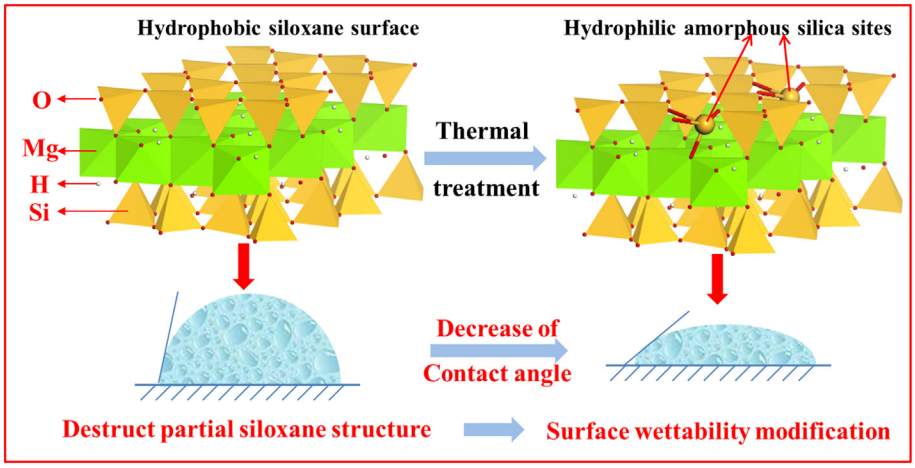

Fig. 10. Schematic representation of thermal treatment of talc for surface wettability modification.

existence of amorphous silica transformed from the destruction of siloxane in calcined talc.

With temperature increasing, especially up to 1300 K, the vibration strength for all the atoms increases. As it continues to absorb energy, some atoms even displace out of the equilibrium position in talc structure due to excessive amount energy uptake from environment of high temperature. Thus the bond length, bond angle is getting abnormal, and the silica tetrahedron structure becomes distorted and finally transformed into amorphous silica. These occurrences of disordered structure and amorphous state result in the decrease of the symmetry of the siloxane structure at talc surface, leading to the enhancement of the polarity at talc surface. As a consequence, the promoted polarity on clay surface leads to a relatively strong affinity of water molecules, resulting in the improvement of hydrophilicity on talc surface after thermal treatment.

3.4. Mechanism and schematic illustration for surface wettability modification of talc

Taken the above results into consideration together, it turned out that thermal treatment is an easy and fast way to modify surface wettability of talc. Through thermal treatment, the symmetrical siloxane structure on clay surface transforms into amorphous silica, the hydrophobic component decreases and the polarity improves, thus gives rise to the enhancement of hydrophilicity on talc surfaces. High temperature environment provides excessive energy thus the atoms move out of the equilibrium position in siloxane structure, the silica tetrahedron structure becomes distorted and finally transformed into amorphous silica. With the increase of thermal treatment time, more and more nonpolar siloxane transformed into polar amorphous silica, the talc surfaces showed a more and more strong affinity to water molecules. As a consequence, it is reasonable that the surface wettability of talc is promoted after thermal treatment. This mechanism of surface wettability modification is schematically depicted, as shown in Fig. 10. This destruction of siloxane structure in clay minerals may have enormous potential application in surface wettability modification due to its easiness, convenience and uniform modification features.

4. Conclusions

It has been found that thermal treatment is an easy and convenient method for the uniform surface wettability modification of clay minerals practically and theoretically in this work. And modification mechanism of this method is to transform hydrophobic siloxane structure on clay mineral surfaces into hydrophilic amorphous silica through calcination. Some atoms displace out of the equilibrium position because thermal treatment provides excess kinetic energy for the vibration of the atoms in talc, leading to the disorder of symmetrical silica tetrahedron and the occurrence of the amorphous phase. The destruction of siloxane symmetry and enhancement of polarity give rise to the relatively strong affinity to water molecules and leads to a hydrophilic basal surfaces of talc. This novel surface wettability modification method of clay mineral may have tremendous potential in taking better advantages of clay minerals.

Acknowledgements

The financial supports to this work from the National Natural Science Foundation of China under the projects Nos. 51674183 and 51874220 are gratefully acknowledged. This research is also supported by the Natural Science Foundation of Hubei Province of China (2018CFB468).

References

Adpakpang, K., Patil, S.B., Oh, S.M., Kang, J.H., Lacroix, M., Hwang, S.J., 2016. Effective chemical route to 2D nanostructured silicon electrode material: phase transition from exfoliated clay nanosheet to porous Si nanoplate. Electrochim. Acta 204, 60–68. https://doi.org/10.1016/j.electacta.2016.04.043.

Andrić, L., Terzić, A., Aćimović-Pavlović, Z., Pavlović, L., Petrov, M., 2014. Comparative kinetic study of mechanical activation process of mica and talc for industrial application. Compos. Part B Eng. 59, 181–190. https://doi.org/10.1016/j.compositesb.2013.12.003.

Barcelos, I.D., Cadore, A.R., Alencar, A.B., Maia, F.C.B., Mania, E., Oliveira, R.F., Bufon, C.C.B., Malachias, Â., Freitas, R.O., Moreira, R.L., Chacham, H., 2018. Infrared fingerprints of natural 2D Talc and plasmon-phonon coupling in graphene-talc heterostructures. ACS Photon. 5, 1912–1918. https://doi.org/10.1021/acsphotonics.7b01017.

Belgacem, K., Llewellyn, P., Nahdi, K., 2008. Thermal behaviour study of the talc. Optoelectron. Adv. Mater. Rapid Commun. 2, 332–336.

Bonati, A., Merusi, F., Bochicchio, G., Tessadri, B., Polacco, G., Filippi, S., Giuliani, F., 2013. Effect of nanoclay and conventional flame retardants on asphalt mixtures fire reaction. Constr. Build. Mater. 47, 990–1000. https://doi.org/10.1016/j.conbuildmat.2013.06.002.

Borges, R., Macedo Dutra, L., Barison, A., Wypych, F., 2016. MAS NMR and EPR study of structural changes in talc and montmorillonite induced by grinding. Clay Miner. 51, 69–80. https://doi.org/10.1180/claymin.2016.051.1.06.

Brigatti, M.F., Galan, E., Theng, B.K.G., 2006. Chapter 2 structures and mineralogy of clay minerals. Dev. Clay Sci. 1, 19–86. https://doi.org/10.1016/S1572-4352(05)01002-0.

Chen, T., Zhao, Y., Song, S., 2017. Electrophoretic mobility study for heterocoagulation of montmorillonite with fluorite in aqueous solutions. Powder Technol. 309, 61–67. https://doi.org/10.1016/j.powtec.2016.12.086.

Claverie, M., Dumas, A., Carême, C., Poirier, M., Le Roux, C., Micoud, P., Martin, F., Aymonier, C., 2018. Synthetic Talc and Talc-like structures: preparation, features and applications. Chem. A Eur. J. 24, 519–542. https://doi.org/10.1002/chem.201702763.

Cygan, R.T., Liang, J.-J., Kalinichev, A.G., 2004. Molecular models of hydroxide, oxyhydroxide, and clay phases and the development of a general force field. J. Phys. Chem. B 108, 1255–1266. https://doi.org/10.1021/jp0363287.

Du, H., Miller, J.D., 2007. A molecular dynamics simulation study of water structure and

adsorption states at talc surfaces. Int. J. Miner. Process. 84, 172–184. https://doi.org/10.1016/j.minpro.2006.09.008.
Fonseca, A.S., Viana, M., Querol, X., Moreno, N., de Francisco, I., Estepa, C., de la Fuente, G.F., 2015. Ultrafine and nanoparticle formation and emission mechanisms during laser processing of ceramic materials. J. Aerosol Sci. 88, 48–57. https://doi.org/10.1016/j.jaerosci.2015.05.013.
Jamil, N.H., Palaniandy, S., 2011. Comparative study of water-based and acid-based sonications on structural changes of talc. Appl. Clay Sci. 51, 399–406. https://doi.org/10.1016/j.clay.2010.12.006.
Jaynes, W.F., Boyd, S.A., 1991. Hydrophobicity of siloxane surfaces in smectites as revealed by aromatic hydrocarbon adsorption from water. Clay Clay Miner. 39, 428–436. https://doi.org/10.1346/CCMN.1991.0390412.
Kaggwa, G.B., Huynh, L., Ralston, J., Bremmell, K., 2006. The Influence of Polymer Structure and Morphology on Talc Wettability. pp. 3221–3227. https://doi.org/10.1021/la052303i.
Kang, S., Zhao, Y., Wang, W., Zhang, T., Chen, T., Yi, H., Rao, F., Song, S., 2018. Removal of methylene blue from water with montmorillonite nanosheets/chitosan hydrogels as adsorbent. Appl. Surf. Sci. 448, 203–211. https://doi.org/10.1016/j.apsusc.2018.04.037.
Krysztafkiewicz, A., Domka, L., 1997. Surface-modified microporous talcs as fillers of polymers and pigments. J. Mater. Chem. 7, 1655–1659. https://doi.org/10.1039/a700040e.
Larentzos, J.P., Greathouse, J.A., Cygan, R.T., 2007. An ab Initio and Classical Molecular Dynamics Investigation of the Structural and Vibrational Properties of Talc and Pyrophyllite. J. Phys. Chem. C 111, 12752–12759. https://doi.org/10.1021/jp072959f.
Li, X., Peng, K., 2018a. $MoSe_2$/Montmorillonite Composite Nanosheets: Hydrothermal Synthesis, Structural Characteristics, and Enhanced Photocatalytic activity. Minerals 8, 268. https://doi.org/10.3390/min8070268.
Li, X., Peng, K., 2018b. Synthesis of 3D mesoporous alumina from natural clays for confining CdS nanoparticles and enhanced photocatalytic performances. Appl. Clay Sci. 165, 188–196. https://doi.org/10.1016/j.clay.2018.08.017.
Li, X., Peng, K., Chen, H., Wang, Z., 2018. TiO_2 nanoparticles assembled on kaolinites with different morphologies for efficient photocatalytic performance. Sci. Rep. 8, 11663. https://doi.org/10.1038/s41598-018-29563-8.
Lippmaa, E., Maegi, M., Samoson, A., Engelhardt, G., Grimmer, A.R., 1980. Structural studies of silicates by solid-state high-resolution silicon-29 NMR. J. Am. Chem. Soc. 102, 4889–4893. https://doi.org/10.1021/ja00535a008.
Liu, X., Liu, X., Hu, Y., 2014. Investigation of the thermal decomposition of talc. Clay Clay Miner. 62, 137–144. https://doi.org/10.1346/CCMN.2014.0620206.
Liu, K., Stadlbauer, W., Zitzenbacher, G., Paulik, C., Burgstaller, C., 2016a. Effects of surface modification of talc on mechanical properties of polypropylene/talc composites. AIP Conf. Proc. 1713. https://doi.org/10.1063/1.4942323.
Liu, S., Liu, X., Guo, Z., Liu, Y., Guo, J., Zhang, S., 2016b. Wettability modification and restraint of moisture re-adsorption of lignite using cationic gemini surfactant. Colloids Surf. A Physicochem. Eng. Asp. 508, 286–293. https://doi.org/10.1016/j.colsurfa.2016.08.073.
Liu, C., Song, S., Li, H., Li, Y., Ai, G., 2019a. Elimination of the adverse effect of calcite slimes on the sulfidization flotation of malachite in the presence of water glass. Colloids Surf. A Physicochem. Eng. Asp. 563, 324–329. https://doi.org/10.1016/j.colsurfa.2018.12.022.
Liu, C., Zhang, W., Song, S., Li, H., 2019b. A novel method to improve carboxymethyl cellulose performance in the flotation of talc. Miner. Eng. 131, 23–27. https://doi.org/10.1016/j.mineng.2018.11.003.
Liu, C., Zhu, G., Song, S., Li, H., 2019c. Flotation separation of smithsonite from quartz using calcium lignosulphonate as a depressant and sodium oleate as a collector. Miner. Eng. 131, 385–391. https://doi.org/10.1016/j.mineng.2018.11.045.
MacKenzie, K.J.D., Meinhold, R.H., 1994. The thermal reactions of talc studied by 29Si and 25Mg MAS NMR. Thermochim. Acta 244, 195–203. https://doi.org/10.1016/0040-6031(94)80219-X.
Michot, L.J., Villiéras, F., François, M., Yvon, J., Dred, R.L.E., Cases, J.M., 1994. The structural microscopic hydrophilicity of talc. Langmuir 10, 3765–3773. https://doi.org/10.1007/s11284-012-0960-6.
Mierczynska-Vasilev, A., Beattie, D.A., 2013. The effect of impurities and cleavage characteristics on talc hydrophobicity and polymer adsorption. Int. J. Miner. Process. 118, 34–42. https://doi.org/10.1016/j.minpro.2012.11.003.
Nalaskowski, J., Abdul, B., Du, H., Miller, J.D., 2007. Anisotropic character of Talc surfaces as revealed by streaming potential measurements, atomic force microscopy, molecular dynamics simulations and contact angle measurements. Can. Metall. Q. 46, 227–235. https://doi.org/10.1179/cmq.2007.46.3.227.
Okada, K., Ikawa, F., Isobe, T., Kameshima, Y., Nakajima, A., 2009. Low temperature preparation and machinability of porous ceramics from talc and foamed glass particles. J. Eur. Ceram. Soc. 29, 1047–1052. https://doi.org/10.1016/j.jeurceramsoc.2008.07.055.
Pack, S., Kashiwagi, T., Cao, C., Korach, C.S., Lewin, M., Rafailovich, M.H., 2010. Role of surface interactions in the synergizing polymer/clay flame retardant properties. Macromolecules 43, 5338–5351. https://doi.org/10.1021/ma100669g.
Peng, K., Fu, L., Ouyang, J., Yang, H., 2016. Emerging parallel dual 2D composites: natural clay mineral hybridizing MoS_2 and interfacial structure. Adv. Funct. Mater. 26, 2666–2675. https://doi.org/10.1002/adfm.201504942.
Pérez-Maqueda, L.A., Balek, V., Poyato, J., Šubrt, J., Beneš, M., Ramírez-Valle, V., Buntseva, I.M., Beckman, I.N., Pérez-Rodríguez, J.L., 2008. Transport properties and microstructure changes of talc characterized by emanation thermal analysis. J. Therm. Anal. Calorim. 92, 253–258. https://doi.org/10.1007/s10973-007-8819-8.
Polowczyk, I., Kozlecki, T., 2017. Central composite design application in oil agglomeration of talc. Physicochem. Probl. Miner. Process. 53. https://doi.org/10.5277/ppmp170230.
Ptáček, P., Lang, K., Šoukal, F., Opravil, T., Bartoníčková, E., Tvrdík, L., 2014. Preparation and properties of enstatite ceramic foam from talc. J. Eur. Ceram. Soc. 34, 515–522. https://doi.org/10.1016/j.jeurceramsoc.2013.08.007.
Richard Ward, J., 1975. Kinetics of talc dehydroxylation. Thermochim. Acta 13, 7–14. https://doi.org/10.1016/0040-6031(75)80061-X.
Rotenberg, B., Patel, A.J., Chandler, D., 2011. Molecular explanation for why talc surfaces can be both hydrophilic and hydrophobic. J. Am. Chem. Soc. 133, 20521–20527. https://doi.org/10.1021/ja208687a.
Samyn, P., 2013. Wetting and hydrophobic modification of cellulose surfaces for paper applications. J. Mater. Sci. 48, 6455–6498. https://doi.org/10.1007/s10853-013-7519-y.
Schoonheydt, R.A., Johnston, C.T., 2006. Chapter 3 Surface and Interface Chemistry of Clay Minerals. vol. 1. pp. 87–113. https://doi.org/10.1016/S1572-4352(05)01003-2.
Šolc, R., Gerzabek, M.H., Lischka, H., Tunega, D., 2011. Wettability of kaolinite (001) surfaces - Molecular dynamic study. Geoderma 169, 47–54. https://doi.org/10.1016/j.geoderma.2011.02.004.
Tesson, S., Salanne, M., Rotenberg, B., Tazi, S., Marry, V., 2016. Classical polarizable force field for clays: pyrophyllite and Talc. J. Phys. Chem. C 120, 3749–3758. https://doi.org/10.1021/acs.jpcc.5b10181.
Ulian, G., Valdrè, G., 2015. Density functional investigation of the thermophysical and thermochemical properties of talc $[Mg_3Si_4O_{10}(OH)_2]$. Phys. Chem. Miner. 42, 151–162. https://doi.org/10.1007/s00269-014-0708-7.
Underwood, T., Erastova, V., Greenwell, H.C., 2016. Wetting effects and molecular adsorption at hydrated kaolinite clay mineral surfaces. J. Phys. Chem. C 120, 11433–11449. https://doi.org/10.1021/acs.jpcc.6b00187.
Wallqvist, V., Claesson, P.M., Swerin, A., Schoelkopf, J., Gane, P.A.C., 2006. Interaction forces between talc and hydrophobic particles probed by AFM. Colloids Surf. A Physicochem. Eng. Asp. 277, 183–190. https://doi.org/10.1016/j.colsurfa.2005.11.101.
Wang, W., Zhao, Y., Bai, H., Zhang, T., Ibarra-Galvan, V., Song, S., 2018a. Methylene blue removal from water using the hydrogel beads of poly(vinyl alcohol)-sodium alginate-chitosan-montmorillonite. Carbohydr. Polym. 198, 518–528. https://doi.org/10.1016/j.carbpol.2018.06.124.
Wang, W., Zhao, Y., Yi, H., Chen, T., Kang, S., Li, H., Song, S., 2018b. Preparation and characterization of self-assembly hydrogels with exfoliated montmorillonite nanosheets and chitosan. Nanotechnology 29. https://doi.org/10.1088/1361-6528/aa9ba4.
Wesolowski, M., 1984. Thermal decomposition of talc: a review. Thermochim. Acta 78, 395–421. https://doi.org/10.1016/0040-6031(84)87165-8.
Xian, Z., Hao, Y., Zhao, Y., Song, S., 2017. Quantitative determination of isomorphous substitutions on clay mineral surfaces through AFM imaging: a case of mica. Colloids Surf. A Physicochem. Eng. Asp. 533, 55–60. https://doi.org/10.1016/j.colsurfa.2017.08.024.
Yang, H., Du, C., Hu, Y., Jin, S., Yang, W., Tang, A., Avvakumov, E.G., 2006. Preparation of porous material from talc by mechanochemical treatment and subsequent leaching. Appl. Clay Sci. 31, 290–297. https://doi.org/10.1016/j.clay.2005.10.015.
Yehia, A., Al-Wakeel, M.I., 2000. Talc separation from talc-carbonate ore to be suitable for different industrial applications. Miner. Eng. 13, 111–116. https://doi.org/10.1016/S0892-6875(99)00154-5.
Yi, H., Zhang, X., Zhao, Y., Liu, L., Song, S., 2016. Molecular dynamics simulations of hydration shell on montmorillonite (001) in water. Surf. Interface Anal. 48, 976–980. https://doi.org/10.1002/sia.6000.
Yi, H., Jia, F., Zhao, Y., Wang, W., Song, S., Li, H., Liu, C., 2018a. Surface wettability of montmorillonite (001) surface as affected by surface charge and exchangeable cations: a molecular dynamic study. Appl. Surf. Sci. https://doi.org/10.1016/j.apsusc.2018.07.216.
Yi, H., Zhao, Y., Rao, F., Song, S., 2018b. Hydrophobic agglomeration of talc fines in aqueous suspensions. Colloids Surf. A Physicochem. Eng. Asp. 538, 327–332. https://doi.org/10.1016/j.colsurfa.2017.11.017.
Yi, H., Zhan, W., Zhao, Y., Qu, S., Wang, W., Chen, P., Song, S., 2019. A novel core-shell structural montmorillonite nanosheets/stearic acid composite PCM for great promotion of thermal energy storage properties. Sol. Energy Mater. Sol. Cells 192, 57–64. https://doi.org/10.1016/j.solmat.2018.12.015.
Zhang, H., Wang, F., 2014. Analysis of surface wettability of synthetic magnetite. J. Wuhan Univ. Technol. Mater. Sci. Ed. 29, 679–683. https://doi.org/10.1007/s11595-014-0979-3.
Zhang, M., Hui, Q., Lou, X.J., Redfern, S.A.T., Salje, E.K.H., Tarantino, S.C., 2006. Dehydroxylation, proton migration, and structural changes in heated talc: an infrared spectroscopic study. Am. Mineral. 91, 816–825. https://doi.org/10.2138/am.2006.1945.
Zhang, Y., Tang, A., Yang, H., Ouyang, J., 2016. Applications and interfaces of halloysite nanocomposites. Appl. Clay Sci. 119, 8–17. https://doi.org/10.1016/j.clay.2015.06.034.
Zhang, Y., Long, M., Huang, P., Yang, H., Chang, S., Hu, Y., Tang, A., Mao, L., 2017. Intercalated 2D nanoclay for emerging drug delivery in cancer therapy. Nano Res. 3, 1–11. https://doi.org/10.1007/s12274-017-1466-x.